APPLICATION OF CFD FOR TRANSIENT MULTIPHASE FLOW AND REACTION MODELLING IN A RISER

N. NOVIA, M. S. RAY, and V. K. PAREEK

Chemical Engineering Department, Curtin University of Technology

GPO Box U1987, Perth 6845, Western Australia

ABSTRACT

A commercial CFD code FLUENT 6.2 was used to simulate three-dimensional, transient multiphase flow and the reaction model in FCC riser reactors under various operating conditions. The conservation equations of mass, momentum and energy together with the equation of turbulence, and chemical species for each phase were solved using the Eulerian-Eularian approach. The three-lump kinetic model was assumed in order to simulate cracking reactions occurring in the FCC riser reactors. The model demonstrated the capability of the commercial CFD model to describe and predict the flow field in the riser reactor. The model also predicts the temperature, the heats of reactions and yield of gasoline along the riser height.

NOMENCLATURE

C_D Drag coefficient, [-]

C_μ Turbulence constant, [-]

d_s Diameter of solid particles, [m]

e_s Particle collisions coefficient, [-]

g Gravitational acceleration, [m s^{-2}]

g_o Radial distribution function, [-]

H_i Specific enthalpy of ith phase, [J kg^{-1}]

$k_{\Theta s}$ Diffusion coefficient, [kg m^{-1} s^{-1}]

k_i Turbulent kinetic energy, [J kg^{-1}]

P Static Pressure, [N m^{-1}]

P_s Solid Pressure, [N m^{-1}]

$\mathbf{q}_i$ The heat flux, [W m^{-2}]

Re_s Relative Reynolds number, [-]

T_s Solid stress tensor, [Pa]

$\mathbf{U}_i$ Velocity of ith phase, [m s^{-1}]

α Turbulent kinetic energy dissipation rate, [m^2 s^{-3}]

β Solid gas exchange coefficient, [kg m^{-3} s^{-1}]

ρ_i Density of ith phase, [kg m^{-3}]

ε_i Volume fraction of ith phase, [-]

ϵ_i Turbulent dissipation rate, [m^2 s^{-3}]

τ_i Shear stress tensor of ith phase, [N m^{-2}]

γ_s Collisional dissipation of energy, [kg m^{-1} s^{-3}]

Θ_s Granular temperature, [m^2 s^{-1}]

$]\mu_b$ Solid bulk viscosity, [kg m^{-1} s^{-1}]

μ_i Viscosity of ith phase, [kg m^{-1} s^{-1}]

$\mu_{s,dill}$ Solid phase dilute viscosity, [kg m^{-1} s^{-1}]

μ_t Turbulent viscosity, [kg m^{-1} s^{-1}]

INTRODUCTION

Numerous research groups have studied the hydrodynamics multiphase flow and reaction kinetics in a riser-reactor both computationally and experimentally. Pekediz et al. (1997) conducted the experiment to calculate the heats of catalytic cracking in the riser. De Wilde et al. (2005) observed multiphase flow mixing in the inlet zone of the riser.

One dimensional plug flow model (Froment and Bischoff, 1990) is not able to describe the complex hydrodynamics in the riser. Therefore, many hydrodynamics model of gas/solid flow in the riser-reactor has been studied by different modelling approaches (Miller and Gidaspow, 1992, Theologos and Markatos, 1993, Benyahia et al., 2000, Pareek et al., 2003, Tsuo and Gidaspow, 1990). However, most of the researchers did not consider ether turbulent flow or catalytic cracking reactions in their model. The catalytic cracking reaction kinetics in two-dimensional model for the FCC process has been proposed by Benyahnia et al. (2003). Furthermore, three-dimensional flow model and the accurate analysis of the flow field are very important to provide the advanced understanding of phenomena in the riser.

Computational fluid dynamics (CFD) provides an analysis and understanding of the complex phenomena in the riser of an FCC unit. The use of CFD not only reduces time and cost but also provides flow field information in the area where measurements cannot be obtained experimentally. Although CFD models are well developed for single-phase flow, application of CFD for multiphase flow and reaction remains complex. Recently, the commercial CFD code FLUENT 6.2 has focused on simulating multiphase flow and chemical reaction modelling. The computational results demonstrate the capability of the commercial CFD model to describe and predict the flow field in the riser reactor. The model also predicted the temperature, the enthalpy, and the yield of gasoline along the riser height.

CFD MODELLING

The governing conservation equations of fluid flow represent mathematical statements of the conservation laws of mass (continuity), momentum and energy. For reacting flows, the chemical species transport and mixing can be estimated using species-transport equations.

Hydrodynamics Model

Conservation Equations

Continuity equation of phase i (i = gas, solid):

$$\frac{\partial}{\partial t}(\rho_i \varepsilon_i) + \nabla.(\rho_i \varepsilon_i \mathbf{U}_i) = 0 \tag{1}$$

Momentum conservation of phase i (i = gas, solid, $k \neq i$):

$$\frac{\partial}{\partial t}(\rho_i \varepsilon_i \mathbf{U}_i) + \nabla.(\rho_i \varepsilon_i \mathbf{U}_i \mathbf{U}_i) = -\varepsilon_i \nabla P \\ + \nabla.\tau_i + \rho_i \varepsilon_i g - \beta(U_i - U_k) \tag{2}$$

Energy conservation of phase i:

$$\frac{\partial}{\partial t}(\varepsilon_i \rho_i H_i) + \nabla.(\varepsilon_i \rho_i \mathbf{U}_i H_i) = -\varepsilon_i \frac{\partial P}{\partial t} \\ + \boldsymbol{\tau}_i : \nabla \mathbf{U}_i - \nabla.\mathbf{q}_i + S_i \tag{3}$$

Interphase Exchange Equations

Syamlal-O'Brien model for the drag force formulation:

$$\beta = \frac{3}{4} C_D \frac{\varepsilon_s \varepsilon_g}{v_{r,s}^2} \frac{\rho_g}{d_s} \left[\frac{\text{Re}_s}{v_{r,s}}\right] |U_s - U_g| \tag{4}$$

Drag coefficient, C_D is given by:

$$C_D = \left[0.63 + \frac{4.8}{\sqrt{\text{Re}_s / v_{r,s}}}\right]^2 \tag{5}$$

$$\text{Re}_s = \frac{\rho_g d_s |U_s - U_g|}{\mu_g} \tag{6}$$

Pressure of Solids

Solids phase pressure (P_s) consists of a kinetic term and particle collisions term:

$$Ps = (1 + 2(1 + e_s)\varepsilon_s g_0)\varepsilon_s \rho_s \Theta_s = \rho_s \varepsilon_s \Theta_s \\ + 2g_0 \rho_s \varepsilon_s^2 \Theta_s (1 + e_s) \tag{7}$$

The radial distribution function, g_0, is :

$$g_0 = \left[1 - \left[\frac{\varepsilon_s}{\varepsilon_{s,max}}\right]^{1/3}\right]^{-1} \tag{8}$$

Solid Shear Stress

Solid phase bulk viscosity:

$$\mu_b = \frac{4}{3} \varepsilon_s \rho_s d_s g_0 (1 + e_s)\left(\frac{\Theta_s}{\pi}\right)^{1/2} \tag{9}$$

Solid phase shear viscosity:

$$\mu_s = \frac{2\mu_{s,dill}}{(1 + e)g_0}\left[1 + \frac{4}{5}(1 + e_s)g_0 \varepsilon_s\right]^2 \\ + \frac{4}{5}\varepsilon_s \rho_s d_s g_0 (1 + e_s)\left[\frac{\Theta_s}{\pi}\right]^{1/2} \tag{10}$$

Solid phase dilute viscosity:

$$\mu_{s,dil} = \frac{5}{16}\rho_s \varepsilon_s l_s \sqrt{2\pi\Theta_s} \tag{11}$$

$$l_s = \frac{\sqrt{2}}{12}\frac{d_s}{\varepsilon_s} \tag{12}$$

Granular Temperature

$$\frac{3}{2}\frac{\partial}{\partial t}(\rho_s \varepsilon_s \Theta_s) + \nabla.(\rho_s \varepsilon_s U_s \Theta_s) = T_s : \nabla U_s \\ + \nabla.(k_{\Theta s}\nabla \Theta_s) - \gamma_s \tag{13}$$

Difusion coefficient for granular energy, $k_{\Theta s}$:

$$k_{\Theta s} = \frac{2k_{\Theta s,dil}}{(1 + e_s)g_0}\left[1 + \frac{6}{5}(1 + e_s)g_0 \varepsilon_s\right]^2 \\ + 2\varepsilon_s^2 \rho_s d_s g_0 (1 + e_s)\left[\frac{\Theta_s}{\pi}\right]^{1/2} \tag{14}$$

where

$$k_{\Theta s,dil} = \frac{75}{64}\rho_s \varepsilon_s l_s \sqrt{2\pi\Theta_s} \tag{15}$$

Collisional energy dissipation, γ_s, is given by:

$$\gamma_s = 3(1 - e_s^2)\varepsilon_s^2 \rho_s g_0 \Theta_s \left[\frac{4}{ds}\left[\frac{\Theta_s}{\pi}\right]^{1/2} - \nabla \mathbf{U}_s\right] \tag{16}$$

k-ε Turbulence Model

In the k-ε turbulence model, the turbulent viscosity is defined as:

$$\mu_{t,i}^{(t)} = \rho_i \varepsilon_i C_\mu \frac{k_i^2}{\epsilon_i} \tag{17}$$

Turbulent kinetic energy, k, and its rate of dissipation ϵ_i can be derived from the following transport equations:

$$\frac{\partial}{\partial t}(\rho_i \varepsilon_i k_i) + \nabla.(\rho_i \varepsilon_i k_i U_i) = \nabla.\left(\varepsilon_i \frac{\mu_i}{\sigma_k}\nabla k_i\right) \\ + (\varepsilon_i G_k - \varepsilon_i \rho_i \epsilon_i) \tag{18}$$

$$\frac{\partial}{\partial t}(\rho_i \varepsilon_i \epsilon_i) + \nabla.(\rho_i \varepsilon_i \epsilon_i U_i) = \nabla.\left(\varepsilon_i \frac{\mu_i}{\sigma_k}\nabla \epsilon_i\right) \\ + \frac{\epsilon_i}{k}(C_{1\epsilon}\varepsilon_i G_k - C_{2\epsilon}\varepsilon_i \rho_i \epsilon_i) \tag{19}$$

Reaction Kinetics Model

For simplification and less computational effort, the three-lump kinetic scheme was used for description of the catalytic cracking reactions. This scheme considered the gas oil feed converted to gasoline and light gases plus coke, then a part of the gasoline is converted to light gases plus coke. The cracking reaction scheme is given by:

$$A_1 \xrightarrow{K_1} A_2$$
$$K_3 \searrow A_3 \swarrow K_2$$
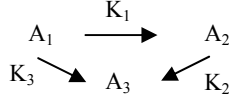
Where A_1 is representative of the gas oil, A_2 is representative of the gasoline, and A_3 is representative of the light gases plus coke. The reaction kinetics is included to the hydrodynamic model by solving the species equation of the components in the form of the reaction rates as follows:

$$\frac{\partial y_1}{\partial t} = -K_1 y_1{}^2 \phi - K_3 y_1{}^2 \phi = -(K_1 + K_3) y_1{}^2 \phi \tag{20}$$

$$\frac{\partial y_2}{\partial t} = K_1 y_1{}^2 \phi - K_2 y_2 \phi = (K_1 y_1{}^2 - K_2 y_2)\phi \tag{21}$$

$$\frac{\partial y_3}{\partial t} = (K_3 y_1{}^2 - K_2 y_2)\phi \tag{22}$$

BOUNDARY CONDITIONS

Figure 1 describes the geometry of the riser. The catalyst and steam are fed from the riser bottom. Gas-oil feedstock enters the riser through four feed nozzles. The riser has diameter between 1 m at the bottom to 1.4 m at the top. The height total of the riser is 7.8 m. In order to reduce the computational effort, and because the riser is symmetric, the riser was split to become a quarter part.

For each simulation, superficial gas and solid velocities were specified. Initially, the riser was filled by 0.56 solid volume fractions at the riser height of 1.6 m from the bottom. The computations started by setting the initial estimate similar to the specified velocities. A constant time step of 0.001 s was used.

Catalyst is fed to the riser with velocity of 0.2 m/s. The volume fraction of catalyst was 40%. The average diameter of catalyst particle was 60 μm, and density of about 1400 kg/m^3. The gas-oil velocity inlet was 10 m/s.
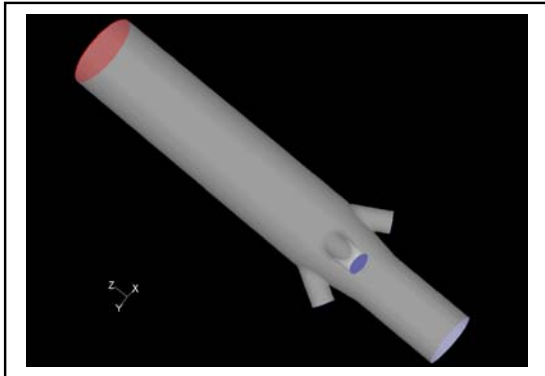
Figure 1: Geometry of the riser (red: outflow; blue: velocity inlet; grey: wall).

COMPUTATIONAL RESULTS

Particle Volume Fractions

Figure 2 shows the time-averaged solids volume fraction along the riser height. The solid volume fraction was higher at the bottom of the riser. After the injection of gas-oil, the solid volume fraction decreased sharply. Then it decreased slowly along the height of the riser. This behaviour is generally observed in the riser (Benyahia et al., 2003). It was suspected that the multiphase mixing due to fast acceleration of particles (gas velocity of about 10 m/s) causes these phenomena. The predicted results indicate that most of the complex mixing phenomena occur in the first 3 to 5 meters of the riser reactor.
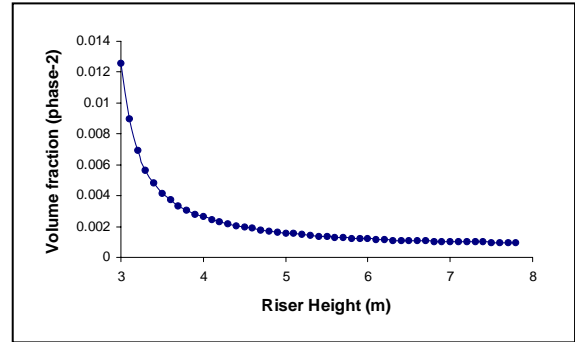
Figure 2: Time-averaged Solid volume fractions along the riser height.

Figure 3 shows the time-averaged radial volume fraction profiles as a function of riser height. The solid volume fraction across the riser diameter decreases with increasing value of the riser height. At the riser height of 3 m, the volume fraction of solid at the wall is higher than at the centre. The core-annular structure was not observed in this model. In addition, Benyahia et al. (2003) have not shown a core-annular flow regime in their two-dimensional model. They concluded that the cracking reactions can effect significantly the radial solid concentration distribution due to the large increase of gas velocity along the riser. Similar trend was observed experimentally by De Wilde et al. (2005). Ranade (1999) also predicted similar profile for the riser diameter of 0.3 and 1.0 m (this work used diameter of 1.4 m). He found a core-annular structure for smaller diameter of 0.06 m.
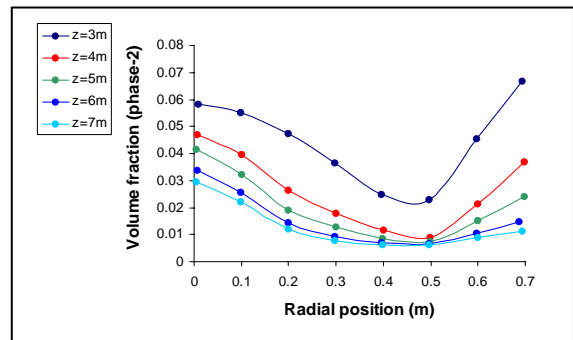
Figure 3: Time-averaged radial solids volume fraction.

3

Solid Velocity Profiles

Figure 4 illustrates the time-averaged velocity profiles of solid along the riser height. The solid velocity increases along the riser height because of the increased amount of hydrocarbon vapours due to the cracking reaction. Catalytic cracking reactions increases moles and cause significant increase in the gas (and catalyst) velocity (Nayak et al., 2005).
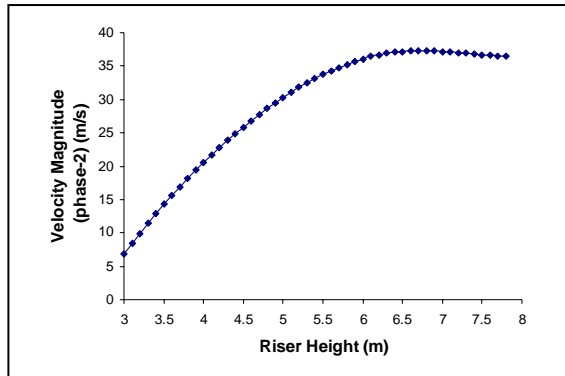
Figure 4: Time-averaged solid velocity profiles along the riser height.

Figure 5 presents the solid velocity profiles at five different cross-sectional z-planes, that is at z = 3 m, z = 4 m, z = 5 m, z = 6 m, and z = 7 m, where z is the axial distance of cross-section from the catalyst inlet. The solid velocity increased with increasing riser height. The minimum velocity is observed at the wall. There is increasing solid velocity at the riser top due to the production of many products such as gasoline and lighter gas. According to Das et al. (2003), the increase in the velocity is caused by the gas-phase pressure at the riser top is lower than at the bottom due to hydrostatic head of the solid. The low pressure allows the gas to expand, thus increasing the solid velocity by the drag force.
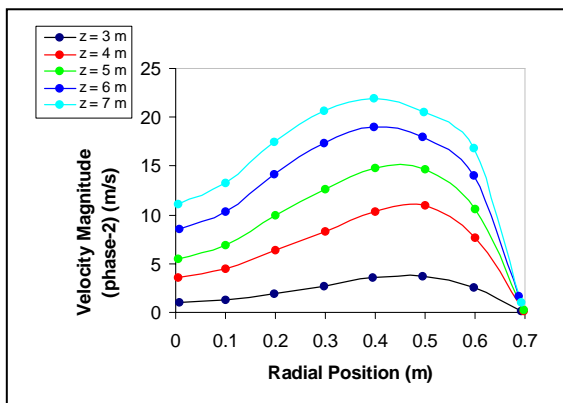
Figure 5: Solid velocity profiles at different riser heights.

Temperature and Enthalpy Profiles

The axial temperature profiles of the solid phase due to the endothermic cracking reactions for various feed inlet temperatures are shown in Figure 6. As expected, the temperature decreased significantly from the bottom to the top of the riser. Furthermore, the maximum temperature drop of the solid phase occurs close to the riser entrance due to higher heat of cracking reactions at the bottom. The

trend of the temperature distribution along the riser height is in agreement with reported results by Pareek et al. (2003).
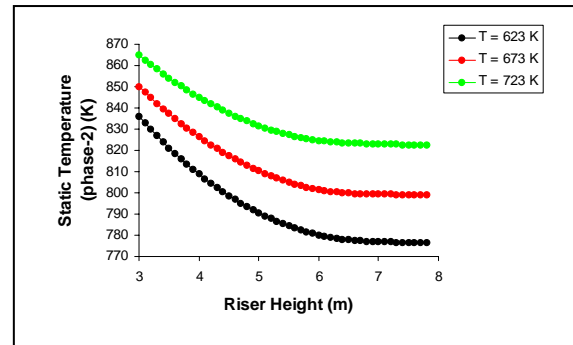
Figure 6: Temperature distribution of solid phase at different height of the riser**.**

Figure 7 shows the enthalpy distributions for various feed inlet temperatures. The enthalpy was higher at the bottom of the riser. Average enthalpy was about 560 to 600 kJ/kg, which is in good agreement with the experimental value reported by Pekediz et al. (1997) and the simulation results reported by Pareek et al. (2003).
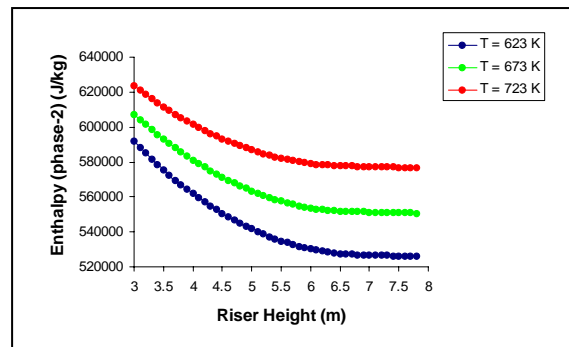
Figure 7: Enthalpy of solid phase at different feed-temperatures.

Mass Fraction of Reactant and Product along the riser height

Figure 8 indicates yields of the cracking reaction along the riser height. There were no reactions with gas oil feed injection under 3 m. The yield of gasoline increased along the height of the riser, however, gas oil declined progressively. The formation of gasoline is most significant at 3 to 5 m from the bottom of the riser. This is due to the higher catalyst activity and the reactivity of gas-oil feedstock at the bottom. Beyond 5 m riser height, the gasoline yield increases but only slightly. These profiles are similar to reported results by several researchers (Benyahia et al., 2003, Pareek et al., 2003, Blasetti and de Lasa, 1997).
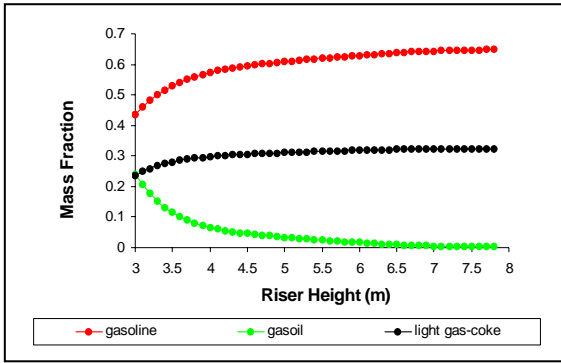
Figure 8: The time-averaged yields distribution along the height of the riser.

Velocity Vector of Particle and Contours of Gasoline Mass Fraction

Figure 9 shows the simulated flow pattern of particle velocity and gasoline mass fraction for the gas velocity and catalyst mass flow rate of 10 m/s and 200 kg/s respectively. Similar flow patterns of particle velocity have been acquired computationally and experimentally by De Wilde et al. (2005).
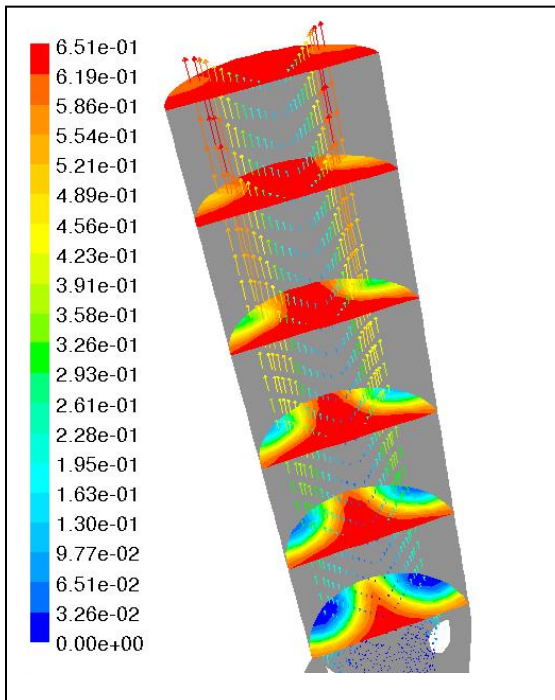
Figure 9: Time-averaged mass fraction of gasoline and solid velocity vectors

Contours of gasoline mass fraction are shown in Figure 9 and 10. It can be seen that a low gasoline mass fraction occurs in the area of the feed inlet nozzles. Interestingly, the complex flow pattern of the riser reactor has an impact on gasoline distribution, especially at the feed injection zone. Higher concentration of gasoline can be found in the upper region (see figure 9). The highest mass fraction of gasoline is about 0.65.
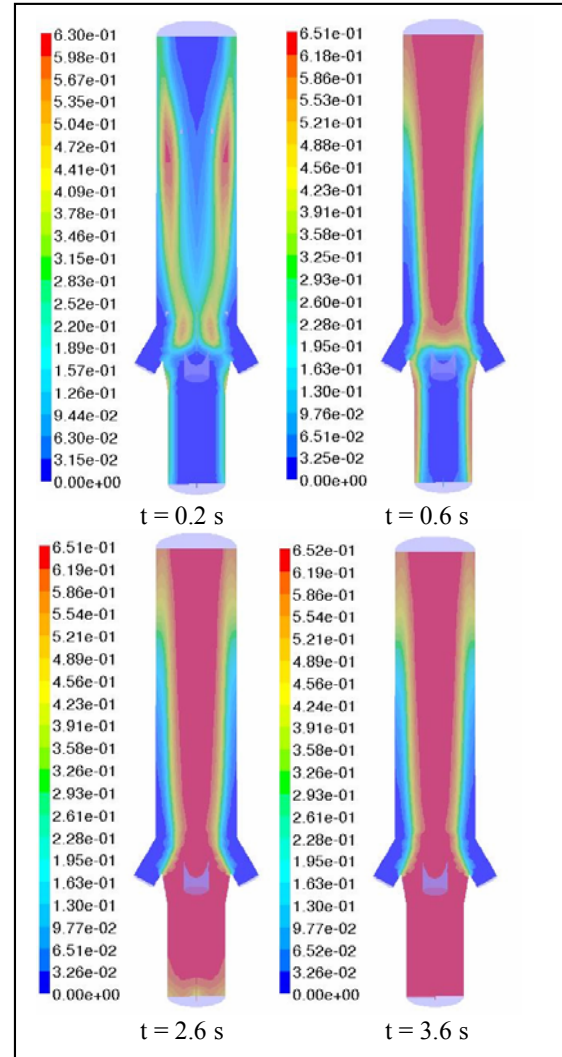
Figure 10: Time-dependent calculations of the contours of gasoline mass fraction for different times (t = 0.2 s; t = 0.6 s; t = 2.6 s; and t = 3.6 s).

CONCLUSIONS

The predicted results indicated that most of the complex mixing phenomena occur in the first 3 to 5 meters of the riser reactor length. The increased amount of hydrocarbon vapours due to the cracking reaction increase the velocity of the gas/solid along the riser height.

Interestingly, the complex flow pattern of the riser reactor has an impact on gasoline distribution, especially at the feed injection zone. A low gasoline mass fraction occurs in the area of the feed inlet nozzles. Higher concentration of gasoline can be found in the upper region of the riser. The gasoline formation is most significant between 3 to 5 m from the bottom of the riser. This is due to the higher catalyst activity and the reactivity of gas-oil feedstock at the bottom.

The maximum temperature drop of the solid phase occurs close to the riser entrance because of the higher heat of cracking reactions at the bottom.

REFERENCES

Benyahia, S., Arastoopour, H., Knowlton, T. M. and Massah, H. (2000), *Simulation of particles and gas flow behavior in the riser section of a circulating fluidized bed using the kinetic theory approach for particulate phase*, Powder Technol.*,* 112**,** 24-33.

Benyahia, S., Ortiz, A. G. and Paredes, J. I. P. (2003), *Numerical analysis of a reacting gas/solid flow in the riser section of an industrial fluid catalytic cracking unit*, International Journal of Chemical Reactor Engineering*,* 1**,** 1-11.

Blasetti, A. and de Lasa, H. (1997), *FCC riser unit operated in the heat-transfer Mode: Kinetic Modeling*, Ind. Eng. Chem. Res.*,* 36**,** 3223-3229.

Das, A. K., Baudrez, E., Marin, G. B. and Heynderick, G. J. (2003), *Three-dimensional simulation of a fluid catalytic cracking riser reactor*, Ind. Eng. Chem. Res.*,* 42**,** 2602-2617.

De Wilde, J., Van Engelandt, G., Heynderickx, G. J. and Marin, G. B. (2005), *Gas-solids mixing in the inlet zone of a dilute circulating fluidized bed*, Powder Technol.*,* 151**,** 96-116.

Froment, G. F. and Bischoff, K. B. (1990), *Chemical Reactor Analysis and Design*, Wiley, New York.

Miller, A. and Gidaspow, D. (1992), *Dense, vertical gas-solid flow in a pipe*, AIChE J.*,* 38**,** 1801-1815.

Nayak, S. V., Joshi, S. L. and Ranade, V. V. (2005), *Modeling of vaporization and cracking of liquid oil injected in a gas-solid riser*, Chem. Eng. Sci.*,* 60**,** 6049-6066.

Pareek, V. K., Adesina, A. A., Srivastava, A. and Sharma, R. (2003), *Modeling of a non-isothermal FCC riser*, Chem. Eng. J.*,* 92**,** 101-109.

Pekediz, A., Kraemer, D. W., Blasetti, A. and de LASA, H. (1997), *Heats of catalyctic cracking. Determination in a Riser Simulator*, Ind. Eng. Chem. Res.*,* 36**,** 4516-4522.

Ranade, V. V. (1999), *Modelling of gas-solid flows in FCC riser reactors: flully developed flow*, Second International Conference on CFD in Minerals and Process Industries**,** 77-82.

Theologos, K. N. and Markatos, N. C. (1993), *Advanced modeling of fluid catalytic cracking riser-type reactors*, AIChE J.*,* 39**,** 1007-1017.

Tsuo, Y. P. and Gidaspow, D. (1990), *Computation of flow patterns in circulating fluidized beds*, AIChE J.*,* 36**,** 885-896.